Available online at www.sciencedirect.com
ScienceDirect
Journal of Power Sources 171 (2007) 778–782
JOURNAL OF POWER SOURCES
www.elsevier.com/locate/jpowsour

Short communication

Corrosion protection of 304 stainless steel bipolar plates using TiC films produced by high-energy micro-arc alloying process

Y.J. Ren, C.L. Zeng *

State Key Laboratory for Corrosion and Protection, Institute of Metal Research, Chinese Academy of Sciences, 62 Wencui Road, Shenyang 110016, China

Received 3 May 2007; received in revised form 13 June 2007; accepted 15 June 2007
Available online 23 June 2007

Abstract

Metallic bipolar plates look promising for the replacement of graphite due to higher mechanical strength, better durability to shocks and vibration, no gas permeability, acceptable material cost and superior applicability to mass production. However, the corrosion and passivation of metals in environments of proton exchange membrane fuel cell (PEMFC) cause considerable power degradation. Great attempts were conducted to improve the corrosion resistance of metals while keeping low contact resistance. In this paper, a simple, novel and cost-effective high-energy micro-arc alloying process was employed to prepare compact titanium carbide as coatings for the type 304 stainless steel bipolar plates with a metallurgical bonding between the coating and substrate. It was found that TiC coating increased the corrosion potential of the bare steel in 1 M H_2SO_4 solution at room temperature by more than 200 mV, and decreased significantly its corrosion current density from 8.3 $\mu A\,cm^{-2}$ for the bare steel to 0.034 $\mu A\,cm^{-2}$ for the TiC-coated steel. No obvious degradation was observed for the TiC coatings after 30-day exposure in solution.

Keywords: Proton exchange membrane fuel cell; Metallic bipolar plate; Type 304 stainless steel; High-energy micro-arc alloying technique; TiC coating; Corrosion

1. Introduction

Proton exchange membrane fuel cell (PEMFC) is a power generation device that converts hydrogen and oxygen (or air) to electricity with water as the only byproduct, and thus has received wide attention due to its reduced emissions, high power density and low operating temperatures. Bipolar plate is an important multifunctional component of PEMFC, and accounts for about 80% of total weight and 45% of stack cost [1]. Bipolar plates perform as the current conductors between cells, facilitate water and thermal management through the cell, and distribute and separate the cathodic and anodic reactant gases. The plates must be of inexpensive, lightweight and must be easily manufactured for commercial applications of PEMFC. The main materials investigated to date for bipolar plates include graphite, metal and graphite polymer composites. Currently, the most commonly used bipolar plate material is graphite or its composites which have low surface contact resistance and high corrosion resistance. Unfortunately, graphite and graphite composites are brittle and permeable to gases, and thus cannot be machined to be thin plates with gas channels on each side. Considerable attentions were recently given to metallic bipolar plates due to their high electrical conductivity, acceptable material cost, high strength, no gas permeability, and applicability to mass production. Moreover, metallic materials can be easily machined to be thin plates with the flow channels, thus significantly reducing the volume and weight of PEMFC. Metals investigated to date mainly include stainless steel, aluminium, titanium and nickel. The main disadvantage of metallic bipolar plates exposed to the acidic and humid environments usually containing SO_4^{2-}, Cl^-, F^- ions, etc., and reactant gases inside the PEMFC is their dissolution or passivation. The corrosion can cause the formation of a passive surface layer which increases the contact resistance, while the metal dissolution can contaminate the membrane electrode. The passivation/dissolution of metallic bipolar plates would cause considerable power degradation. In order to balance the corrosion rate and the surface contact electric resistance, one solution is to coat the metallic bipolar plates with protective coatings. Coatings should be conductive and protect effectively the base metal from exposing to

* Corresponding author. Tel.: +86 24 23904553; fax: +86 24 23893624.
E-mail address: clzeng@imr.ac.cn (C.L. Zeng).

0378-7753/$ – see front matter © 2007 Elsevier B.V. All rights reserved.
doi:10.1016/j.jpowsour.2007.06.075

corrosive species. Many coatings such as noble metals, metal carbides/nitrides/borides exhibit both excellent corrosion resistance and high electrical conductivity. Considerable attempts have been conducted to develop conductive coatings for metallic bipolar plates, mainly including carbon-based and metal-based [2–7]. Recently, Tawfik et al. [8] presented a comprehensive review of the research work conducted on metal bipolar plates to prevent corrosion while maintaining a low contact resistance. Carbon-based coatings include graphite, conductive polymer, diamond-like carbon, and organic self-assembled monopolymers. Metal-based coatings studied to date mainly include noble metals and metal nitrides/carbides. The high price of noble metals coatings is an obstacle to their commercial application in PEMFC. Metal nitrides/carbides commonly prepared by sputtering or ion plating, show better potentiality for application in PEMFC than noble metals coatings. However, these coating processes are prone to pinhole defects, which are detrimental to the corrosion resistance of the coatings [5]. Brady et al. [9] have recently developed a preferential thermal nitridation process to form pinhole-free CrN/Cr_2N coatings on a Ni–Cr alloy plate. These coatings exhibit excellent corrosion resistance and negligible contact resistance. Viable techniques for coating metallic bipolar plates are still under development.

High-energy micro-arc alloying (HEMAA) technique is a simple and cost-effective technique to produce pinhole-free coatings. A metallurgical bonding between the coating and the substrate alloy can be realized by using this technique. In this study, TiC coatings with a minimum porosity were prepared on the type 304 stainless steel using HEMAA, and the corrosion behavior in H_2SO_4 solution was also examined.

2. Experimental

Type 304 stainless steel (304SS) was used as the substrate alloy. The steel plates were cut into specimens of 10 mm × 10 mm, followed by grinding with 600-grit SiC paper and degreasing with acetone. In order to produce a compact coating on 304SS, we have considered a novel process based on HEMAA technique to prepare conductive TiC coatings for metal bipolar plates. This method normally can produce high-quality diffusion coatings at a lower cost, with a minimal thermal distortion or microstructural changes of the substrate due to low energy transfer involved in the HEMAA process. Moreover, the obtained coatings exhibit high resistance to spallation due to the metallurgical bonding between the coating and the alloy substrate. In the present study, a commercial TiC rod was used as the electrode for the deposition of TiC coatings. To avoid heating and oxidation during deposition, the substrate area was kept at room temperature by a strong jet of argon gas. With a succession of pulse discharge depositing operation under the conditions of low voltage and high frequency, a TiC layer with a thickness less than 1 μm was deposited on 304SS. Specimens with and without TiC coatings were embedded in epoxy resign, with an exposed surface of 1 cm^2.

A conventional three-electrode system was used for the electrochemical measurements, with a platinum sheet as the counter electrode and a saturated calomel electrode (SCE) as the reference electrode. All electrochemical measurements were conducted in 1 M H_2SO_4 solution at room temperature with PAR 2273 Potentiostat/Galvanostat. Potentiodynamic polarization was undertaken with a potential scan rate of 20 mV min^{-1} after 1 h immersion in solution. To investigate the performance and stability of TiC coatings, potentiostatic polarization was also conducted at the potential of +600 mV (SCE), close to the working potential of the cathode for a PEMFC [10]. Electrochemical impedance measurements were carried out between 0.01 Hz and 100 kHz during 30-day immersion in solution. The amplitude of input sin-wave voltage was 5 mV.

Scanning electron microscopy (SEM) coupled with energy dispersive X-ray microanalysis (EDX) and X-ray diffraction (XRD) were used to characterize the coatings.

3. Results and discussion

3.1. Characterization of TiC coatings

Fig. 1 shows the typical surface morphology of TiC coating deposited on 304SS using HEMAA technique. The coating surface was compact, and exhibited the molten appearance which is the characteristics of HEMAA process. EDX analysis confirmed the presence of Ti and C. Further analysis by XRD (Fig. 2) indicated the formation of TiC on the steel surface.

3.2. Electrochemical polarization measurements

Fig. 3 shows the potentiodynamic polarization curves for the TiC-coated 304SS and the bare 304SS in 1 M H_2SO_4 aqueous solution at room temperature, respectively. TiC coating was in passive state at the corrosion potential (E_{corr}), whereas 304SS was in active state at E_{corr}. The passive current density for the TiC-coated steel was lower than that for the bare steel by more than two orders of magnitude. E_{corr} and the corrosion current density (I_{corr}) for 304SS were −89 mV (SCE) and 8.3 μA cm^{-2},

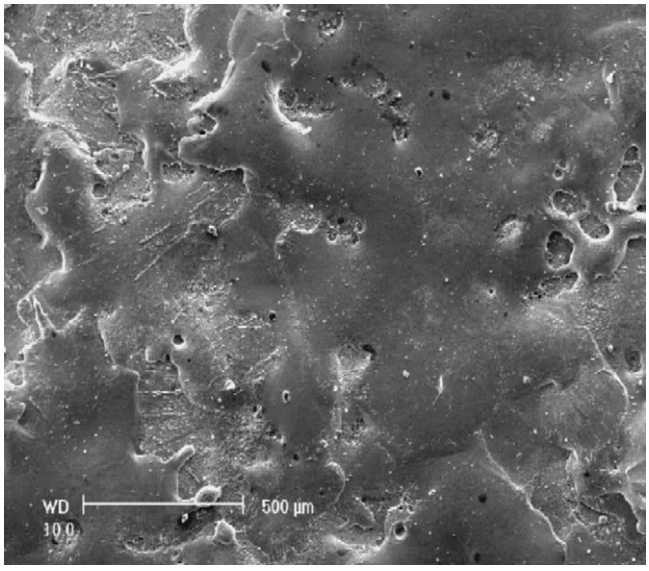

Fig. 1. Surface morphology of TiC film on 304 stainless steel.

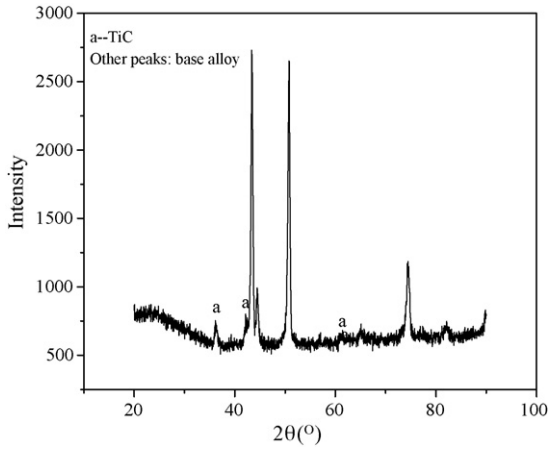

Fig. 2. X-ray diffraction pattern for the TiC-coated 304 stainless steel.

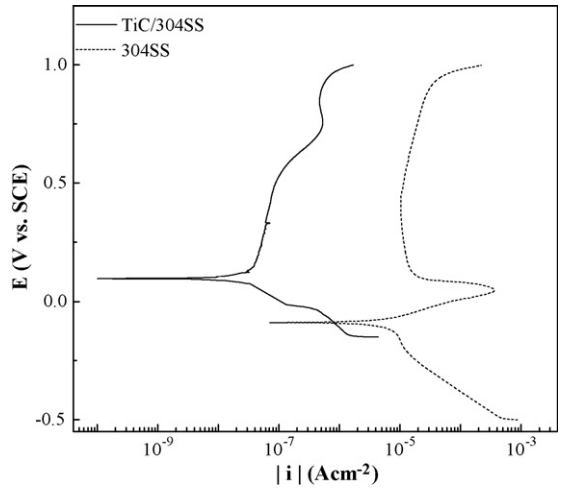

Fig. 3. Potentiodynamic polarization curves for the TiC-coated and the bare 304SS in 1 M H_2SO_4 solution at 25 °C.

respectively, while E_{corr} and I_{corr} for the TiC-coated steel were 98 mV (SCE) and 0.034 μA cm^{-2}, respectively. It is evident that TiC coating significantly increased the corrosion resistance of 304SS in 1 M H_2SO_4 solution.

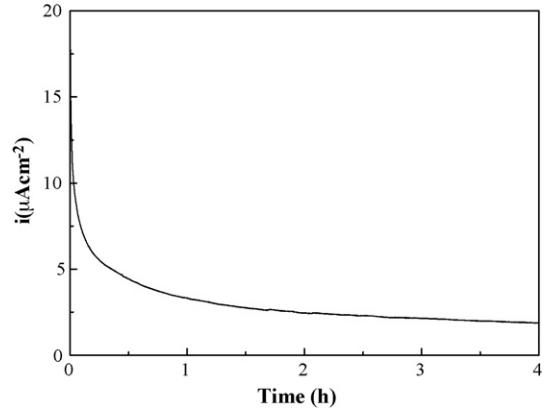

Fig. 4. Polarization current vs. time curve for the TiC-coated steel potentiostatically polarized at +600 mV (SCE) in 1 M H_2SO_4 solution at 25 °C.

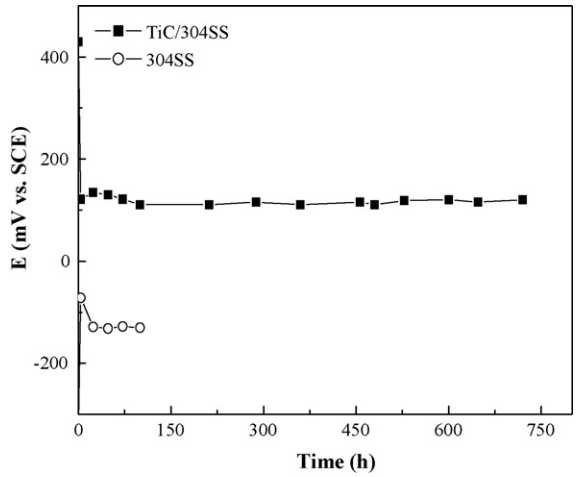

Fig. 5. Open circuit potential vs. time curves for the TiC-coated and the bare 304SS in 1 M H_2SO_4 solution at 25 °C.

Fig. 4 shows the potentiostatic polarization curve for the TiC-coated steel in 1 M H_2SO_4 solution at +600 mV (SCE). The polarization current density of TiC coating specimen decreased significantly to a steady value of around 3.7 μA cm^{-2}. No degradation was observed after potentiostatic measurements for 4 h, indicating the high stability of TiC coating at the cathode working potential of PEMFC.

3.3. Corrosion at free corrosion potentials

The high stability of TiC coating in 1 M H_2SO_4 solution was also confirmed by the measurements of E_{corr} versus time curves for the TiC-coated and the bare steels, respectively, as shown in Fig. 5. E_{corr} for the TiC-coated steel was higher than that for the bare steel by more than 200 mV. Moreover, it remained nearly constant during 30-day immersion in solution, with a stable value of about 120 mV (SCE), suggesting a steady corrosion. The obvious fluctuations of E_{corr} were not observed for TiC coatings during exposure up to 30 days. This is different from the behavior observed for the steel covered with TiN coating prepared by physical vapor deposition (PVD) [5]. Due to the inward penetration of corrosive species to the substrate alloy along the coating pinholes or defects, and the subsequent passivation of the steel, E_{corr} for the TiN-coated steel fluctuated greatly in the initial exposure. It is evident that a more compact coating could be obtained by HEMAA technique than by PVD. Thus, TiC coatings prepared by HEMAA can hinder more effectively the corrosion species from reaching the substrate alloy than PVD coatings.

3.4. Electrochemical impedance measurements

Fig. 6 shows the typical Nyquist and Bode plots for 304SS in 1 M H_2SO_4 solution after various exposure times. The Nyquist plots were composed of two depressed semi-circles. An equivalent circuit of Fig. 7a was proposed to fit the impedance plots. In Fig. 7a, R_s represents the electrolyte resistance, R_f and C_f represent the resistance and the capacitance of porous corro-

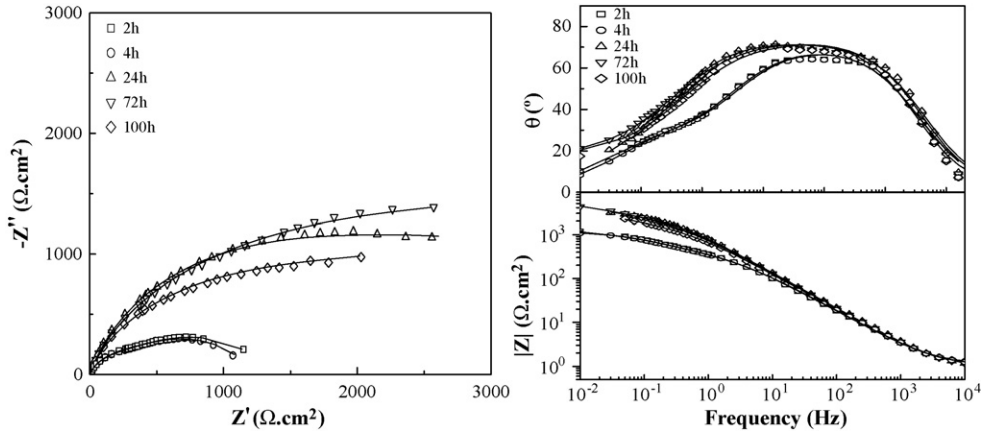

Fig. 6. Nyquist and Bode plots for 304SS after immersion in 1 M H_2SO_4 solution for various times at 25 °C. Symbol: experimental data and line: fitted data.

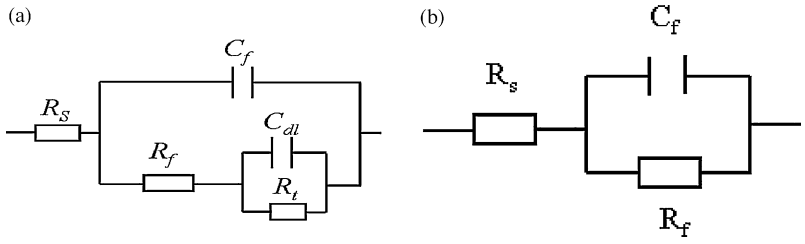

Fig. 7. Equivalent circuits representing the corrosion of the bare 304SS (a) and the TiC-coated 304SS (b) in 1 M H_2SO_4 solution at room temperature, respectively.

sion product layer on the alloy surface, respectively, R_t and C_{dl} are the charge transfer resistance and the double layer capacitance. In the fitting procedure, both C_f and C_{dl} were replaced with constant phase element (CPE) Q_f and Q_{dl}, respectively. The impedance of CPE is expressed as

$$Z_{CPE} = \frac{1}{Y_0}(j\omega)^{-n}$$

where ω is the frequency, Y_0 the admittance magnitude of CPE, n the exponential term, and $0 < n < 1$. Y_f and n_f, Y_{dl} and n_{dl} are constants representing the elements Q_f and Q_{dl}, respectively.

Differing from the bare steel, the Nyquist plots for the TiC-coated steel were composed of a large semi-circle, as shown in Fig. 8. In Bode plots, $\log|Z|$ is linear with frequency $\log f$ and the phase angle is close to 75° in the middle and low frequency region less than 100 Hz, which are characteristic of a predominantly capacitive behavior. Thus, the electrochemical impedance spectra for the TiC-coated steel just reveal the impedance responses from TiC coating due to the absence of coating pinholes as the inward diffusion paths of test solution. Therefore, an equivalent circuit (Fig. 7b) of solution resistance R_s in series with a parallel circuit of interface capacitance C_f and interface resistance R_f was proposed to fit the impedance spectra.

The equivalent circuits of Fig. 7 fitted the experimental date very well, as shown in Figs. 6 and 8, respectively. Tables 1 and 2 give the fitted results of the impedance spectra for the corrosion of the bare and TiC-coated steels, respectively. Table 1 indicated that R_f for 304SS increased significantly to 2692 Ω cm² after exposure of 24 h and then tended to decrease, while Y_f

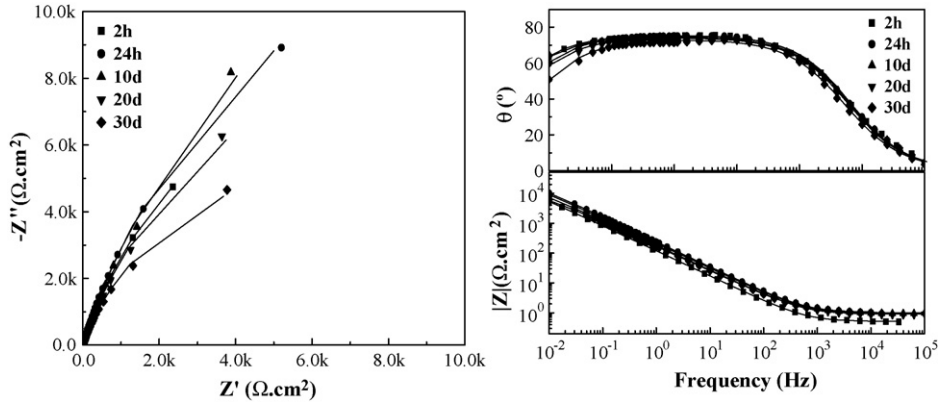

Fig. 8. Nyquist and Bode plots for the TiC-coated 304SS after immersion in 1 M H_2SO_4 solution for various times at 25 °C. Symbol: experimental data and line: fitted data.

Table 1
Fitted results of impedance spectra for the corrosion of 304SS in 1 M H_2SO_4 solution at 25 °C after various exposure times

Time (h)	R_s ($\Omega\,cm^2$)	Y_f ($\times10^{-4}\,\Omega^{-1}\,cm^{-2}\,s^{-n}$)	n_f	R_f ($\Omega\,cm^2$)	Y_{dl} ($\Omega^{-1}\,cm^{-2}\,s^{-n}$)	n_{dl}	R_t ($\Omega\,cm^2$)
2	1.04	3.22	0.80	403	1.78×10^{-3}	0.58	969
4	1.05	3.13	0.80	387	1.67×10^{-3}	0.62	846
24	0.94	2.06	0.81	2692	1.88×10^{-3}	0.60	2744
72	0.97	2.56	0.82	2171	8.78×10^{-4}	0.64	3354
96	1.14	2.67	0.82	1530	1.16×10^{-3}	0.55	3094

Table 2
Fitted results of impedance spectra for the corrosion of the TiC-coated 304SS in 1 M H_2SO_4 solution at 25 °C after various exposure times

Time (h)	R_s ($\Omega\,cm^2$)	Y_f ($\Omega^{-1}\,cm^{-2}\,s^{-n}$)	n_f	R_f ($\times10^{-4}\,\Omega\,cm^2$)
2	0.51	1.80×10^{-3}	0.84	2.473
24	1.04	9.05×10^{-4}	0.84	3.769
48	1.06	9.18×10^{-4}	0.84	3.291
96	0.91	9.38×10^{-4}	0.83	4.538
120	1.01	1.00×10^{-3}	0.83	4.760
240	0.99	1.03×10^{-3}	0.83	4.407
360	0.90	1.10×10^{-3}	0.83	2.971
480	0.90	1.22×10^{-3}	0.83	2.538
720	0.98	1.74×10^{-3}	0.82	1.414

decreased slightly in the initial times and then tended to increase with exposure time, probably relating to the change of the thickness and dielectric constant of the porous corrosion product layer formed on 304SS during active dissolution. The values of n_f related to the surface roughness of the corrosion product layer almost remained constant, suggesting no significant change in the surface area of the corrosion layer. Y_{dl} and n_{dl} did not change regularly with time, whereas the corrosion resistance R_t increased with time, indicating the decrease in the corrosion rate of the steel. From Table 2, it is seen that Y_f for the TiC-coated steel increased slightly with exposure time, except for corrosion of 2 h, while R_f decreased from initial 2.473×10^4 to $1.414\times10^4\,\Omega\,cm^2$ after 720 h immersion in 1 M H_2SO_4 solution, probably relating to a certain degradation of the films. Additionally, n_f also almost remained constant. It is evident that TiC coatings exhibit high stability in H_2SO_4 solution, and are effective barriers to the inward penetration of test solution, and thus reduce significantly the corrosion of the substrate alloy.

4. Conclusions

TiC coatings with a minimum porosity were successfully deposited on 304SS using high-energy micro-arc technique, with a metallurgical bonding between the coating and the substrate. 304SS could not passivate spontaneously in 1 M H_2SO_4 solution at room temperature, while TiC coating was in passive state at the corrosion potential. TiC coating increased the open circuit potential of 304SS by more than 200 mV, and decreased clearly its corrosion current density from 8.3 $\mu A\,cm^{-2}$ for the bare steel to 0.034 $\mu A\,cm^{-2}$ for the coated steel. TiC coating did not go through degradation under the condition of potentiostatic polarization at +600 mV (SCE), close to the cathode operation potential of PEMFC, and exhibited high stability during 30-day immersion. TiC coatings prepared by HEMAA are more compact than by PVD, and thus act as more effective barriers to the inward penetration of corrosive species.

The on-going research work includes the contact electric resistance and the corrosion resistance of TiC coatings in actual PEMFC conditions.

References

[1] Kobayashi, Int. J. Hydrogen Energy 29 (2004) 985.
[2] R.L. Borup, N.E. Vanderborgh, Mater. Res. Soc. Symp. Proc. 393 (1995) 151.
[3] A.S. Woodman, E.B. Anderson, K.D. Jayne, M.C. Kimble, American Electroplaters and Surface Finishes Society 1999, AESF SUR/FIN'99 Proceedings, June 21–24, 1999.
[4] P.L. Hentall, J.B. Lakeman, G.O. Mepsted, P.L. Adcock, J.M. Moore, J. Power Sources 80 (1999) 235.
[5] M.C. Li, S.Z. Luo, C.L. Zeng, J.N. Shen, H.C. Lin, C.N. Cao, Corros. Sci. 46 (2004) 1369.
[6] E.A. Cho, U.S. Jeon, S.A. Hong, I.H. Oh, S.G. Kang, J. Power Sources 142 (2005) 177.
[7] A. Hermann, T. Chaudhuri, P. Spagnol, Int. J. Hydrogen Energy 30 (2005) 1297.
[8] H. Tawfik, Y. Hung, D. Mahajan, J. Power Sources 163 (2007) 755.
[9] M.P. Brady, K. Weisbrod, I. Paulauskas, R.A. Buchanan, K.L. More, H. Wang, M. Wilson, F. Garzon, L.R. Walker, Scr. Mater. 50 (2004) 1017.
[10] H. Wang, J.A. Turner, J. Power Sources 128 (2004) 193.